Available online at www.scholarsresearchlibrary.com

Scholars Research Library

Scholars Research Library

European Journal of Applied Engineering and Scientific Research, 2014, 3 (4):40-47
(http://scholarsresearchlibrary.com/archive.html)

ISSN: 2278 – 0041
CODEN(USA): EJAEAJ)

Quantitative SEM analysis of $(Ba_{0.77}Ca_{0.23})(Re_{0.02}Ti_{0.98})O_3$ ceramics for Re= Pr, Dy, La

A. Moquim and Manas R. Panigrahi

Electroceramics Lab, Department of Physics, School of Applied Sciences, KIIT University, Bhubaneswar, Odisha, India

---

ABSTRACT

*In this paper we are presenting a unique analysis from SEM (scanning electron microscope) of a materials for the first time. No such literature is available in the scientific domain. Here we are presenting quantitative parameters of the sem micrographs in terms of aspect ratio, roundedness, distribution profile of grains, surface profile, deviation etc. So far, only the morphology, **agglomeration**, presence of secondary phases etc. have been reported by several researchers from the scanning electron microscopic studies. Here, it is an opportunity to present a different kind of study **of** $(Ba_{0.77}Ca_{0.23})(Re_{0.02}Ti_{0.98})O_3$ ceramics for Re= Pr, Dy, La**,** prepared by mixed oxide route from the same characterization in a unconventional way.*

Keywords: Aspect ratio; roundedness; distribution profile of grains; surface profile; deviation.

INTRODUCTION

$BaTiO_3$ can form solid solutions with other perovskite ferroelectric-like $CaTiO_3$. Ca-doped $BaTiO_3$ ($Ba_{1-x}Ca_xTiO_3$) crystals are considered to be one of the foremost potential candidates for the lead-free electro-optic modulators and memory devices [1]. Ca^{2+} replaces Ba^{2+} in $BaTiO_3$ to form tetragonal BCT solid solutions. Ca^{2+} has a smaller ionic radius than Ba^{2+}. However, it has been pointed out that the Ca ions in (Ba, Ca) TiO_3 might have greater atomic polarizability. The possible origin of the giant dielectric properties and the dielectric relaxation behavior were explained based on the electrically heterogeneous microstructure [2]. Earlier this type of study is presented [3-4] **in** $Ba_{1-x}Re_x$ TiO_3 ceramics. But, in this study we are representing the microstructure due to effect of 0.02 wt% of rare earth on the solid solubility limit of calcium doped $BaTiO_3$ ceramics.

A solid does not flow and hence centre of the powder particles remain fixed in the matrix determined by the compaction process and subsequently the bridge between them cannot change. This lead to an equilibrium structure. Sintering is an irreversible process in which the free energy decrease is brought about by a decrease in surface area. Ceramography is used to quantify the grain size and shape. The grain size and other microstructural characteristics are all dependent on the processing conditions and methods used to fabricate the ceramic. The mean diameter of the grains in a microstructure can be defined as the diameter of a circle with the same area as the mean grain area in a ceramographic cross section. Other techniques used for the measurements are Martin, Feret and Nassenstein measurement method [5]. Theory says that a specimen measured by all the above methods is likely to have different grain size because the methods do not measure the exact same thing. The shape of the grains can be statistically quantified by dimensionless ratios called shape factors. The shape factor ratios include axial lengths, areas, perimeters and moments of grain shapes. Aspect ratio is the ratio of the largest diameter of a grain to the smallest diameter and roundedness of the grain relates the area of a grain to its perimeter.

MATERIALS AND METHODS

Rare earth, Re= Pr, Dy, La modified (BaCa) TiO_3 ceramics were prepared just above its solid solubility limit i.e. $Ba_{0.77}Ca_{0.23}TiO_3$ by conventional solid state reaction (SSR) technique. Stoichiometric proportionate high purity powders of $BaCO_3$ (99.9% pure Merck), $CaCO_3$(99.9% pure Merck), TiO_2(99.9% pure Merck), Pr_6O_{11}(99.9% pure Merck), Dy_2O_3(99.9% pure Merck), and La_2O_3(99.9% pure Merck) were gounded for more than 6 h with acetone medium in an agate mortar for homogeneous mixing of powders. The composite powder of the compounds was conventionally calcined at 1280℃ for 4 h in an electrical furnace. Then the calcined powders were once again thoroughly mixed and ground for 2 h, mixed with 2wt.% of polyvinyl alcohol (PVA) as binder and pressed into disk-shaped pellets of 10 mm diameter and finally the green ceramics were sintered at 1320℃ for 6 h. Scanning electron microscopy (SEM) of Jeol JSM 6480LV was used for the observation of the microstructure of the ceramics. An electron beam of 10 kV and 57 µA was used for the SEM study. The average grain size was estimated through scanning electron microscope.

Theory:

Amongst the different stages of ceramic processing, greenbody formation from the monosized sub-micron powder into a well-compacted shape is of great concern. Greenbody formation concern with the powder particle agglomeration leads to particle binding under the appraisal of force in order to form strong greenbody.

In ceramics large grain boundary charges are expected to attract or repel ions or charge defects from within the ceramics. So grain boundaries are sinks for impurities and some types of lattice vacancy. Grain boundary movement has a dominating influence on the fabrication of high density ceramics by sintering. If one grain is surrounded by four other grains, then the reference grain shrinks and if one grain is surrounded by eight other grains the reference grain grows outward into the surrounding.

Inverse of the grain radius determines the excess pressure which in turn determines the number of excess vacancies below the surface. So the movement rate of the grain boundary is

Grain growth rate $\alpha \frac{1}{r_{gb}} \equiv \frac{1}{d_g}$, where d_g is grain diameter.

RESULTS AND DISCUSSION

The SEM micrograph in Fig.1 shows that, the grain size **is** almost equiaxed, dense having clear grain boundary. There is no evidence of secondary phase. The euhedral microstructures are clearly seen in the micro graphs. The roundedness and the aspect ratios of almost all the samples are found to be closer to one for the largest grain. The mean diameter of the grains in a microstructure can be defined as the diameter of a circle with same area as the mean grain area in a ceramographic cross section, which would be equivalent to the diameter of a sphere with the same volume as the mean grain volume. Grain sizes in a ceramographic section are distributed around at least one mean value. The diameter varies substantially within each grain where the maximum diameter might be an order of magnitude greater than the minimum and the actual size varies among neighboring grains in a ceramic. Properties that are sensitive to grain shape such as toughness of ceramics, and effectiveness of abrasive particles are correlated to shape factors. Grain shape may have some effect on strength and fracture mode of the ceramic [6]. Two dimensional shape factors do not necessarily corresponds well to actual grain shape in three dimension. The grain shape are tabulated in Table-1. Porosity decreases strength, because pores reduce the true crosssection area of a member and also pores act as stress-concentrating notches [7]. In this study , we found that the porosity of all the specimens is <6% (approx.), which means that the pores are discrete and match with the porosity thumb rule. The euhedral microstructure of the ceramics is similar to the shape of the Bravais lattice cell and is clearly observed in Fig. 1. It was reported that the driving forces for densification and grain growth are comparable in magnitude, both being proportional to the reciprocal grain size. The compositional EDS analysis shows the consistency amongst different participating elements.

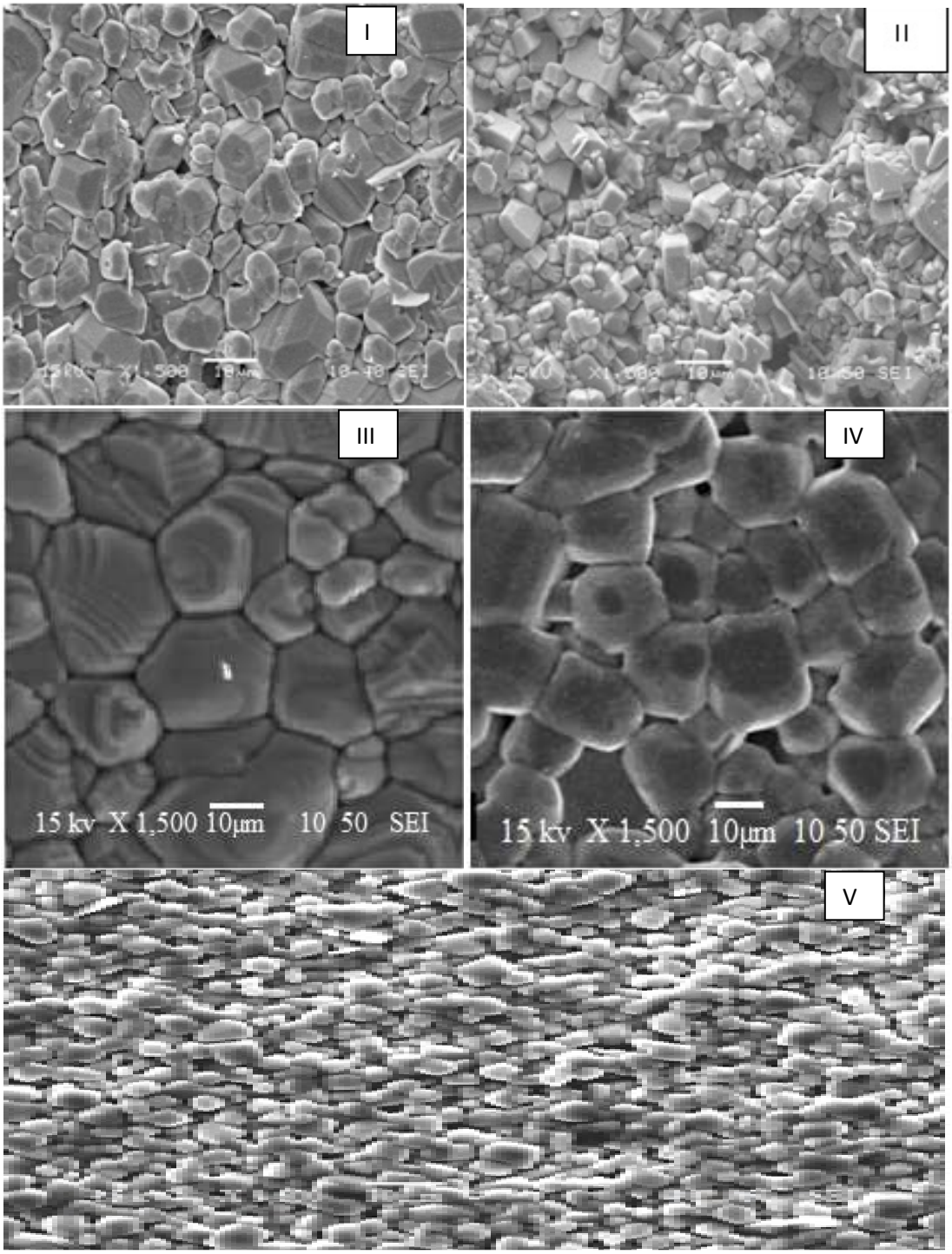

Fig. 1: SEM micrographs of (I) $BaTiO_3$, (II) $Ba_{0.77}Ca_{0.23}TiO_3$ and (III),(IV), and (V) for $(Ba_{0.77}Ca_{0.23})(Re_{0.02}Ti_{0.98})O_3$ ceramics for Re= Pr, Dy, La.

Table-1 shows that aspect ratio and roundedness of the samples decreases gradually with Ca and Dy doped $BaTiO_3$, but, it increases when it is doped with La and Pr. Though the variation is very small, it speaks about the increasing and decreasing nature of the grain size when it is doped with the studied materials in that particular range at the solid solubility limit of Ca modified $BaTiO_3$ ceramics. Standard deviation is a measure of grain sizes around the mean and generally incorporates grain diameter, plane of intersection with the grain and the actual size. Standard deviation precludes quantified accuracy and statistical characterization and its advantage is that, it is fast, easy and well suited to ball-park figure situation [8]. Thin sections are not easily quantified because many grains overlap, the smaller grains are obscured and the plane of focus is distorted in z-**dimension**. In our analysis the large deviation may be due to the small quantity of intersections, combined with a variety of grain sizes when several fields are counted.

Table-1: Quantitative analysis of $(Ba_{0.77}Ca_{0.23})(Re_{0.02}Ti_{0.98})O_3$ ceramics from its SEM micrographs.

Sample	Ar	R	Grain size(um)	Mean	RGB Mean	W	h	Dev.
$BaTiO_3$	.7841	1.005	4.25	134.567	47.90	7.61	7.61	92.366
$Ba_{.77}Ca_{.23}TiO_3$	.7277	1.002	5.13	179.438	12.46	6.54	6.15	31.81
$(Ba_{.77}Ca_{.23})(Dy_{.02}Ti_{.98})O_3$	.7253	1.001	9.53	66.997	248.86	12.55	9.98	21.643
$(Ba_{.77}Ca_{.23})(La_{.02}Ti_{.98})O_3$	.882	0.997	4.41	114.075	247.80	5.1	5.1	38.504
$(Ba_{.77}Ca_{.23})(Pr_{.02}Ti_{.98})O_3$	.9066	1.001	15.62	47.90	47.90	16.40	18.00	92.366

The distribution of grain sizes in all the samples are shown in the profile plot in fig.2 using **image J**. Distribution of grain sizes shows that, in sample $BaTiO_3$, **between** 12.5 µm to 16 µm distance the share of gray scale is comparatively less while at distances 10 µm and 17.5 µm it is comparatively large. In the second samples i.e. $Ba_{0.77}Ca_{0.23}TiO_3$, at distances upto 6 µm the distribution of gray scale is larger and beyond 9 µm it is very less within 130-150. But, with Pr modified $Ba_{0.77}Ca_{0.23}TiO_3$ the plot profile is almost uniform throughout the studied range. At the same time it is observed that, profile of the 4th and 5th samples i.e. Dy and La modified $Ba_{0.77}Ca_{0.23}TiO_3$ ceramics the profile is almost uniformly distributed which is very appreciably observed in the La modified $Ba_{0.77}Ca_{0.23}TiO_3$ whose mean lies within 130 gray scale. Dy modified $Ba_{0.77}Ca_{0.23}TiO_3$ ceramics shows that the profile is very smooth and the share % is distributed within a small range of 15 to 20 gray scale.

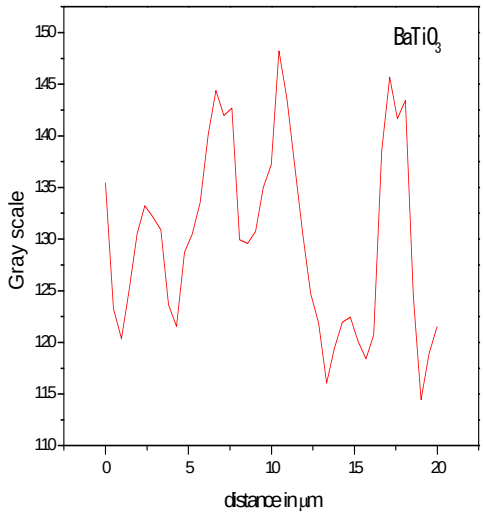

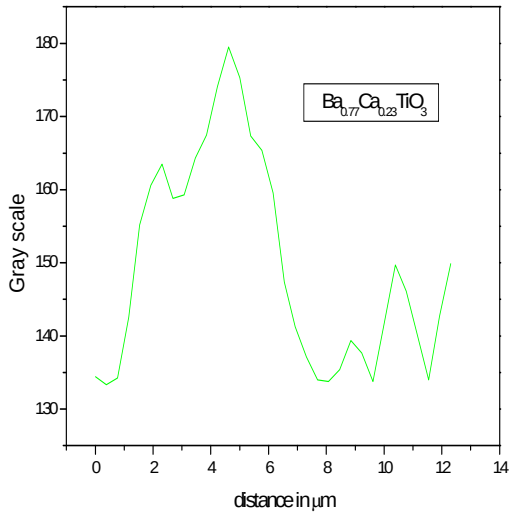

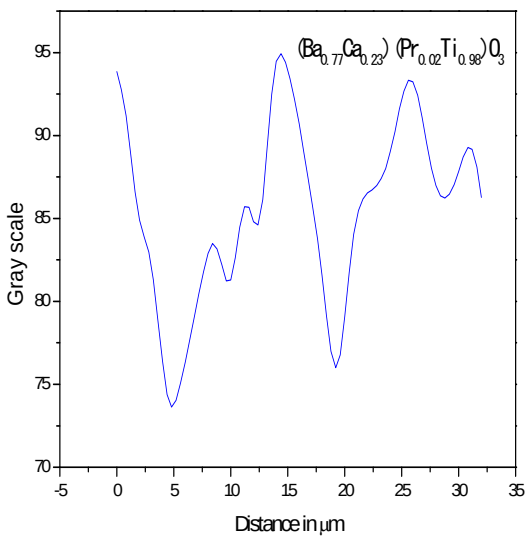

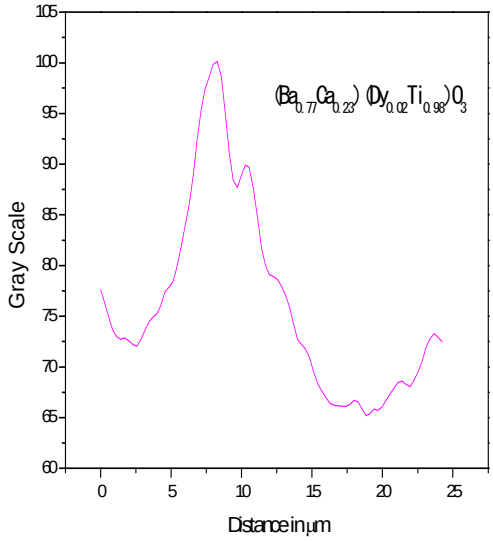

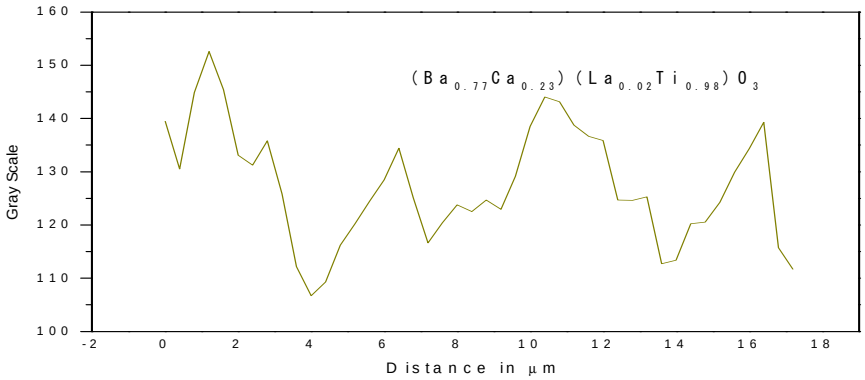

Fig. 2: Profile plot of $BaTiO_3$, $Ba_{0.77}Ca_{0.23}TiO_3$ and $(Ba_{0.77}Ca_{0.23})(Re_{0.02}Ti_{0.98})O_3$ ceramics for Re= Pr, Dy, La.

The EDX analysis shows that, for all the doping concentrations, the theoretical wt% of the elements is more or less the same with the experimental wt% calculated from the EDX **compositional analysis**. This shows a consistency of the elemental wt% present in the green ceramics and is tabulated in table-2. Thus it can be said that, the processing technique is acceptable as the composite materials are seen in single phase both theoretically and experimentally.

Table-2: Elemental analysis of $BaTiO_3$, $Ba_{0.77}Ca_{0.23}TiO_3$ and $(Ba_{0.77}Ca_{0.23})(Re_{0.02}Ti_{0.98})O_3$ ceramics for Re= Pr, Dy, La.

Sample	Element	Theoretical wt%	Experimental wt%
$BaTiO_3$	Ba	*58.29*	63.91
	Ti	*20.52*	18.03
	O	*20.58*	18.06
$(Ba_{0.77}Ca_{0.23})TiO_3$	Ba	*50.15*	*53.62*
	Ti	*22.70*	*20.44*
	O	*22.77*	*21.91*
	Ca	*4.37*	*4.03*
$(Ba_{0.77}Ca_{0.23})(Pr_{0.02}Ti_{0.98})O_3$	Ba	*49.72*	*51.57*
	Ti	*22.06*	*18.88*
	O	*22.57*	*23.53*
	Ca	*4.33*	*3.98*
	pr	*1.33*	*2.04*
$(Ba_{0.77}Ca_{0.23})(Dy_{0.02}Ti_{0.98})O_3$	Ba	*49.62*	*51.98*
	Ti	*22.01*	*18.77*
	O	*22.52*	*25.39*
	Ca	*4.32*	*3.82*
	Dy	*1.53*	*1.04*
$(Ba_{0.77}Ca_{0.23})(La_{0.02}Ti_{0.98})O_3$	Ba	*49.73*	*51.53*
	Ti	*22.06*	*17.99*
	O	*22.57*	*24.49*
	Ca	*4.33*	*3.92*
	La	*1.31*	*2.07*

Fig.3(A) gives the shape factors of $BaTiO_3$, $Ba_{0.77}Ca_{0.23}TiO_3$ and $(Ba_{0.77}Ca_{0.23})(Re_{0.02}Ti_{0.98})O_3$ ceramics for Re= Pr, Dy, La, in terms of aspect ratio(A_R) and Roundedness(R). From the figure it is observed that the roundedness almost remains constant at around 1, which indicate the equiaxed nature of the grain. Here, it is different from the micrograph, because 2D micrographs is different from the 3D quantitative analysis. In fig. 3(B) it is seen that, the grain size increases when $BaTiO_3$ is modified with Ca^{2+} at its solid solubility limit, but, **when** this material is modified at its B site with rare earth element like Dy, La and Pr, the grain size increases both for Dy and Pr, and simultaneously, it decreases when it is modified with La. This may be attributed to their molecular weight. The grain size is largest for the Pr modified $BaCaTiO_3$ and at the same time its aspect ratio is also largest amongst the studied range. This nature also attributed to the highest dielectric constant of the material because of the above mentioned nature[9]. Fig. 5 shows the histogram of different elements in the studied range and analyzed area in the micrograph.

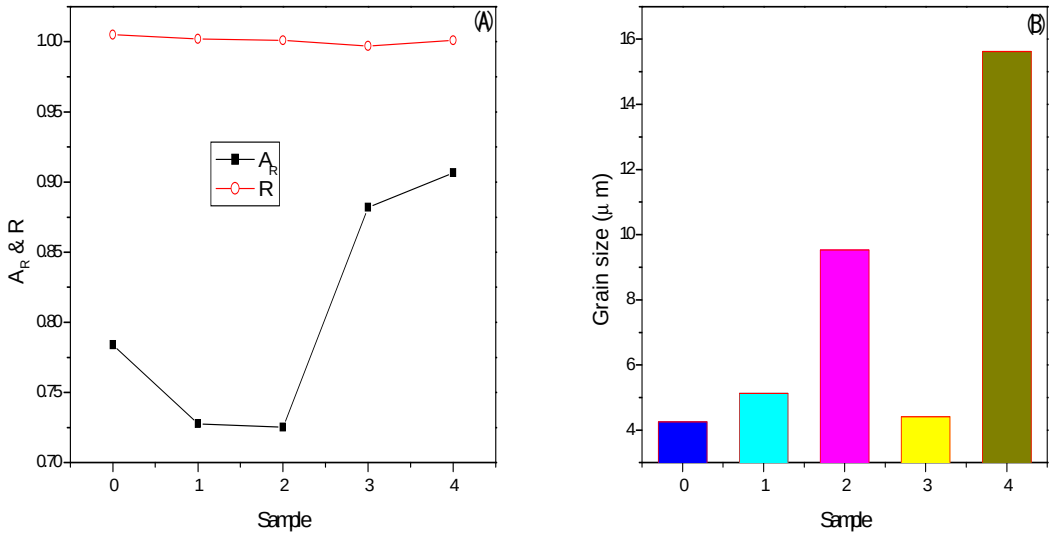

Fig.3(A) Shape factor (B) Grain Size of $BaTiO_3$, $Ba_{0.77}Ca_{0.23}TiO_3$ and $(Ba_{0.77}Ca_{0.23})(Re_{0.02}Ti_{0.98})O_3$ ceramics for Re= Pr, Dy, La which corresponds to 0,1,2,3,4 and 5 samples respectively.

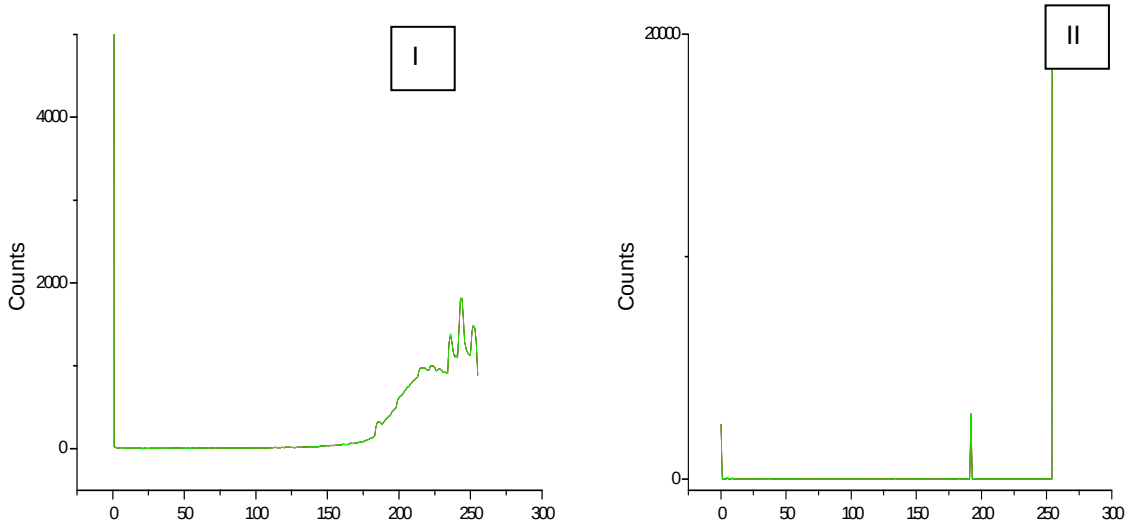

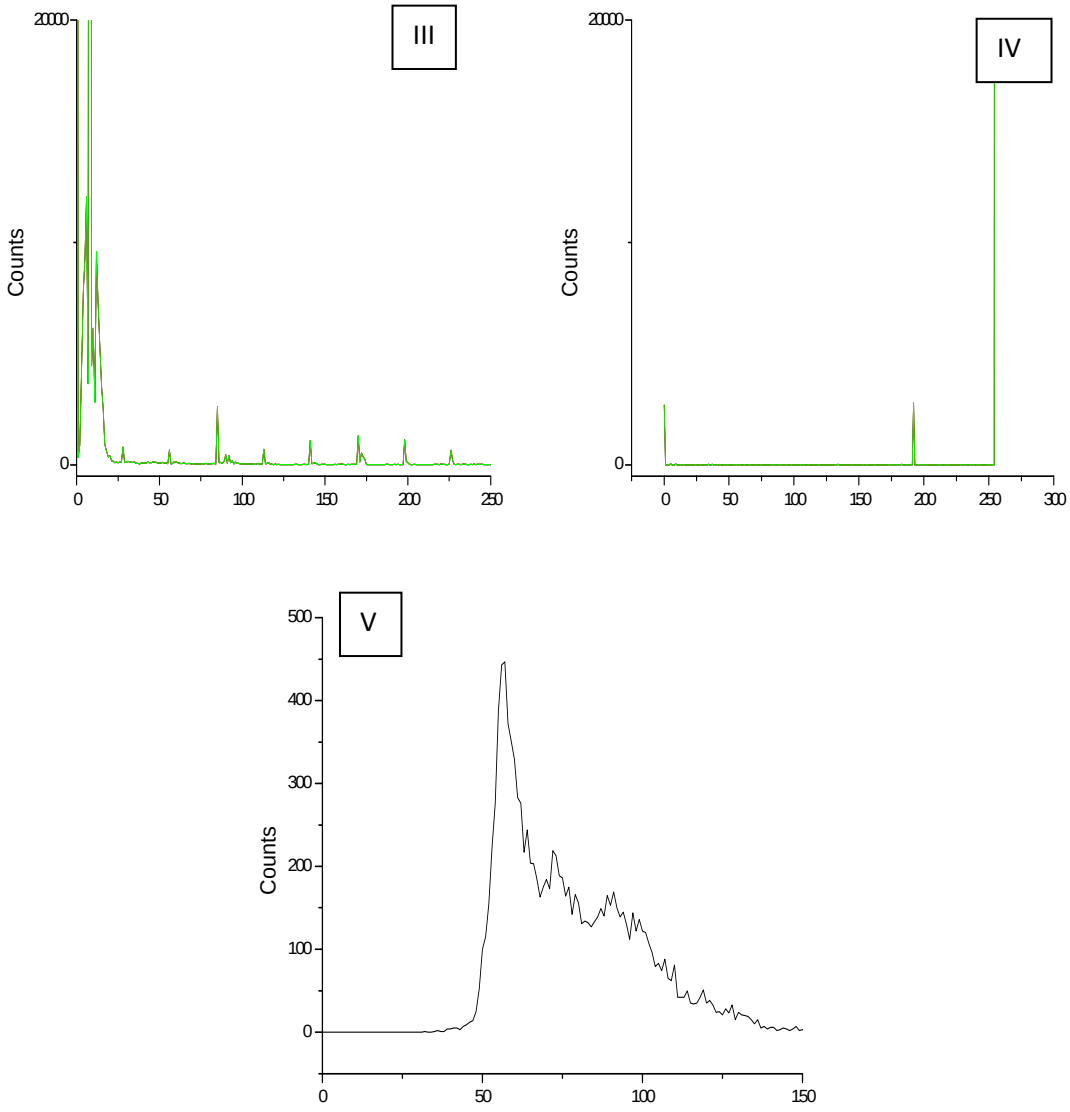

Fig. 4: Histogram of $BaTiO_3$, $Ba_{0.77}Ca_{0.23}TiO_3$ and $(Ba_{0.77}Ca_{0.23})(Re_{0.02}Ti_{0.98})O_3$ ceramics for Re= Pr, Dy, La, for I,II,III,IV and V respectively.

CONCLUSION

In this paper we tried to quantify the SEM micrographs of rare earth modified $(Ba_{0.77}Ca_{0.23})TiO3$ at its solid solubility limit. Though many researchers have studied rare earth modified ceramics for different purposes, but for the first time we have reported the quantitative parameters of $(Ba_{0.77}Ca_{0.23})(Re_{0.02}Ti_{0.98})O_3$ ceramics for Re= Dy, La, Pr, which gives an insight to the understand the process and materials parameters of the ceramics. The analysis shows that the grains are almost equiaxed. Grain size and the shape factor of the ceramics can be controlled by the processing techniques and materials parameters which may be useful in different applications starting from MLCC to electronic applications.

REFERENCES

[1] Veenhuis H, Borger T, Piethmann K, **(2000).** *Appl. Phys. B:. Laser Opt.* 70 797.
[2] Thongbai P, Putasaeng B, Yamwong T , Maensiri S, **(2012).** *Materials Research Bulletin*, 47: 2257–2263.
[3] Panigrahi M.R, Panigrahi S, **(2009)**. *Physica B: Condensed matter* 404: 4267–4272
[4] Panigrahi M.R, Panigrahi S, **(2010)**. *International Journal of Material Science*, 5: 651--656.
[5] Underwood E.E, **(1970)**. Quantitative Stereology, Addition Wesley Publishing Co., Reading, MA.
[6] Rice R.W, **(2000).** Mechanical properties of ceramics and composites, Marcel Dekker, Inc. 127-244.
[7] MacCrone R.K., **(1977).** Properties and microstructure, Academic press, 199-381.

[8] Russ J.C., Dehoff R.T.,**(2000)**. Practical steoreology, 2nd ed. Kluwer Academic, 45-57.
[9] Liu Z.Y, Li X.M, Wu J.Q, **(2012).** *J. Am. Ceram. Soc*. 95 476.